THE KINETICS RELATING CALCIUM AND FORCE IN SKELETAL MUSCLE

R. B. STEIN, J. BOBET, M. N. OĞUZTÖRELI, AND M. FRYER
Departments of Physiology and Mathematics, University of Alberta, Edmonton, Canada T6G 2H7; and School of Physiology and Pharmacology, University of New South Wales, Kensington, N.S.W., Australia 2033

ABSTRACT The kinetics relating Ca^{2+} transients and muscle force were examined using data obtained with the photoprotein aequorin in skeletal muscles of the rat, barnacle, and frog. These data were fitted by various models using nonlinear methods for minimizing the least mean square errors. Models in which Ca^{2+} binding to troponin was rate limiting for force production did not produce good agreement with the observed data, except for a small twitch of the barnacle muscle. Models in which cross-bridge kinetics were rate limiting also did not produce good agreement with the observed data, unless the detachment rate constant was allowed to increase sharply on the falling phase of tension production. Increasing the number of cross-bridge states did not dramatically improve the agreement between predicted and observed force. We conclude that the dynamic relationship between Ca^{2+} transients and force production in intact muscle fibers under physiological conditions can be approximated by a model in which (*a*) two Ca^{2+} ions bind rapidly to each troponin molecule, (*b*) force production is limited by the rate of formation of tightly bound cross-bridges, and (*c*) the rate of cross-bridge detachment increases rapidly once tension begins to decline and free Ca^{2+} levels have fallen to low values after the last stimulus. Such a model can account not only for the pattern of force production during a twitch and tetanus, but also the complex, nonlinear pattern of summation which is observed during an unfused tetanus at intermediate rates of stimulation.

INTRODUCTION

Calcium is an important cofactor in many cellular processes and much effort has gone into attempts to measure intracellular Ca^{2+} ion concentrations in living cells (reviewed by Blinks et al., 1982). Among the best studied systems is skeletal muscle in which Ca^{2+} binds to the protein troponin and enables the interaction between thick myosin-containing filaments and thin actin-containing filaments and the subsequent production of force (e.g., Hibberd and Trentham, 1986; Zot and Potter, 1987).

Despite the impressive advances in the molecular biology of isolated muscle proteins studied in a test tube, the quantitative relation between Ca^{2+} and force in the living cell is still far from being understood. Several noteworthy attempts have been made to model the release and sequestration of Ca^{2+} in muscle cells (Gillis et al., 1982; Cannell and Allen, 1984; Melzer et al., 1986), but the effects of Ca^{2+} on force production have been more elusive. In part this results from the fact that many of the Ca^{2+} indicators (e.g., arsenazo-III, quin 2, fura 2) are very sensitive to movement artifacts so that they cannot be used in functional, contracting muscle cells. However, the photoprotein aequorin is not as limited and published data have been available from frog (Blinks et al., 1978), barnacle (Ashley and Moisescu, 1972), and rat skeletal muscle (Eusebi et al., 1980) for some time.

The purpose of this paper is to test available data from a variety of skeletal muscles in relation to a number of basic questions: (*a*) how complex a model is needed to fit the relation between Ca^{2+} and force adequately? (*b*) Is existing data sufficient to distinguish between models in which Ca^{2+} binding to troponin is rate limiting and those in which some step in the cross-bridge kinetics is rate limiting? (*c*) Can the data distinguish between different orders and degrees of cooperativity in Ca^{2+} binding? In attempting to answer these questions, we will start with simple, but perhaps unrealistic models, and systematically add complexity as required to determine how much the fit to the data is improved. Nonlinear, least mean squares methods will be applied at each stage to optimize the fit of the data to the models.

METHODS

All models considered were evaluated by comparing their predictions with experimental data from rat, barnacle, and frog muscle fibers. Each data set consisted of the time course of force and the associated free Ca^{2+} ion concentration. The fibers had been injected intracellularly with the photoprotein aequorin. The transient light emission after electrical stimulation of the muscle was converted to Ca^{2+} concentrations according to the methods described below.

In one model (Eq. 1.4), standard, linear, least mean squares techniques

Address correspondence to Dr. R. B. Stein, Department of Physiology, University of Alberta, Edmonton, Canada T6G 2H7.

could be applied to obtain the best-fitting parameters (Sokolnikoff and Redheffer, 1958). The other models could not be expressed in this form, and fitting was then done using a gradient-search algorithm as follows: (*a*) initial estimates of the parameters were provided to the algorithm, and the sum of squared errors (variance) between the predicted and observed traces was calculated. (*b*) These parameters were then increased and decreased by 50% one at a time and the errors reassessed. The particular combination of values that produced the greatest reduction in variance was then accepted and the parameters were again varied. When a 50% change in any of the constants no longer produced an improved fit, the size of the step was halved and the procedure was repeated. (*c*) When a variation of 6.25% in the values of the parameters no longer produced any improvement in fit, the algorithm was considered to have converged, and the values of the parameters and the residual variance were recorded. Running the algorithm to greater precision (estimates to within 1.5%) typically improved the variance by only a small amount and did not significantly alter the values of the parameters.

A confidence interval for the best-fitting parameters was calculated by the method of Kawai and Brandt (1980). Briefly, a critical *F*-value was calculated based on the residual variance of the model, the number of fitted data points, and the number of free parameters. The constants were then varied, one at a time, and a new variance calculated. The range of values for a given parameter, which did not increase the error by more than the critical value, provided the 95% confidence interval for the constant. Note that this method may overestimate the accuracy of the computations, because the parameters are not generally an orthogonal set and can interact with one another. Such interactions are not taken into account in the method of Kawai and Brandt (1980).

The agreement between predicted and observed traces was quantified by calculating the root-mean-square (RMS) error between the two traces. To allow comparisons of models across data sets, this error was expressed as a percentage of the standard deviation of the observed trace about its mean. For example, if an observed force trace had a standard deviation of 5 mN about its mean force level and the RMS error of the model predictions from the observed data set was 1 mN, then the residual error was 20%.

In principle, a model can be evaluated by its ability to predict force from Ca^{2+} or Ca^{2+} from force. In practice, convergence was more certain and the residual errors were smaller when force was predicted from Ca^{2+}. In most models the prediction of Ca^{2+} from force required that the force trace be differentiated at least once, a process that magnified any noise present on the force signal and thus yielded greater errors. Conversely, force prediction required integration of the Ca^{2+} trace, a process that tended to reduce the effect of noise. The best-fitting parameters for both force prediction and Ca^{2+} prediction were similar, typically lying within the 95% confidence interval, so that the values obtained for the constants did not depend on the direction of the fitting algorithm. Thus, only the prediction of force from Ca^{2+} will be reported here.

Several different data sets were used to evaluate the models. Sample force and Ca^{2+} traces are shown in Fig. 3 of Results below. One of the authors (M. Fryer) obtained the data from small bundles of rat soleus muscle fibers in Dr. I. Neering's lab. The data shown were collected at 20°C. The data for frog tibialis anterior muscle at 21°C were collected by another of the authors (R. B. Stein) in Dr. John Blinks' lab. All of the traces for rat and frog muscles are the average of at least four trials. Data from barnacle giant muscle fibers at 10–12°C were digitized from the published records of Ashley and Moisescu (1972), as reproduced in Ashley (1978), and from Duchateau and Hainaut (1986).

Light emitted by aequorin was converted to Ca^{2+} ion concentration for the rat using the relationship described by Allen and Blinks (1979). Several potential difficulties can arise from this procedure (Blinks et al., 1982). (*a*) The resting Ca^{2+} levels are contaminated to some extent by the Ca^{2+}-independent level of the light produced by aequorin. (*b*) Because of the nonlinear relation between light and Ca^{2+}, local "hot spots" of Ca^{2+} concentration can distort the total Ca^{2+} estimate. (*c*) The release of light from aequorin is not instantaneous and introduces some delays.

The extent of the delays is known and did not seriously affect the results shown from muscle fibers at room temperature or below. The effect of subtracting off various background levels was tested and did not affect the results qualitatively although the quantitative values of the parameters were changed somewhat (see Results). The effect of local hot spots of Ca^{2+} is the most difficult potential error to estimate, but it probably did not affect our results substantially (see Discussion).

Values from the maximum light emission were not available for the frog data, so Ca^{2+} concentrations were obtained by taking the 2.5th root of the light trace. The values were then scaled to match published, tetanic levels of ~2 μM (Cannell, 1986). For the barnacle data of Ashley and Moisescu (1972), Ca^{2+} concentrations were available from the published curves, although these were based on the assumption that light emission is proportional to the square of Ca^{2+} ion concentration. While this assumption is somewhat in error (Allen and Blinks, 1979), their Ca^{2+} measurements were used here without modification in order that the results from our modeling could be directly compared with theirs. For the barnacle data of Duchateau and Hainaut (1986) data were converted to Ca^{2+} concentration using the 2.5th root of light, as for the frog, and the peak value during the twitch was scaled so that it matched the data of Ashley and Moisescu (1972), which seems to have been gathered under similar conditions. Throughout this paper Ca^{2+} concentrations are expressed in μM and force in mN.

RESULTS

1. Contractions Limited by Calcium Kinetics

Calcium binds to a number of sites in muscle fibers, but the one of most interest here is the binding to the protein troponin. This binding will depend on the concentration of free Ca^{2+} ions, denoted here by the letter c. Let x_0 be the fraction of regulatory sites on troponin without a Ca^{2+} bound and x_1 be the fraction with Ca^{2+} bound. If there is no cooperativity between sites, then the reaction will be as shown in Fig. 1 *A*, where a is the forward rate constant and b the back rate constant governing Ca^{2+} binding. Written as a differential equation, this first order reaction is

$$dx_1/dt = acx_0 - bx_1 \tag{1.1}$$

and from the definition of x_0 and x_1 as fractions,

$$x_0 + x_1 = 1. \tag{1.2}$$

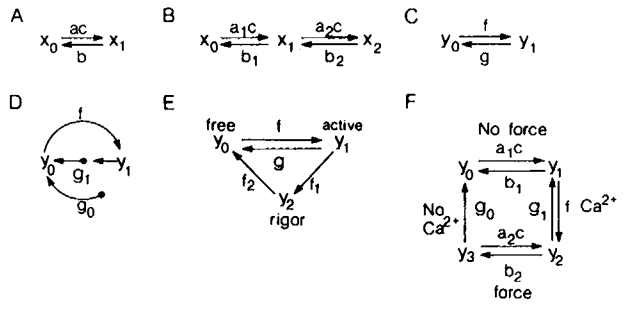

FIGURE 1 Models relating Ca^{2+} transients and force generation considered in this paper. In *A* and *B*, Ca^{2+} kinetics are rate-limiting and Ca^{2+} binding to troponin is either independent (*A*) or sequential (*B*). In *C–E*, cross-bridge kinetics are rate-limiting via a simple two-state model (*C*), a two-state model with a switchable detachment rate constant (*D*), or a three-state model (*E*). In *F*, both Ca^{2+} and cross-bridge kinetics serve to limit force generation. Further details in the text.

The simplest assumption, although probably an unrealistic one which will be removed later, is that there is an instantaneous relation between the troponin molecules with some number n Ca^{2+} ions bound and force production F. Then,

$$F = mx_1^n + o, \tag{1.3}$$

where m is the proportionality constant and o is an offset constant. An offset is included since there may be mechanisms for force production in the muscle other than cross-bridge formation (e.g., passive, parallel, elastic elements).

If $n = 1$ and $x_1 \ll 1$, then Eqs. 1.1–1.3 can be solved for the Ca^{2+} concentration c in terms of the force F. The solution has the form

$$c = pF + q\,dF/dt + r, \tag{1.4}$$

where $p = b/(am)$, $q = 1/(am)$, and $r = -po$. The values of the three free parameters which minimize the least mean square error can then be determined by the standard linear methods (Sokolnikoff and Redheffer, 1958). From these parameters we can determine $b = p/q$ and $o = -r/p$, but a and m always appear in the product form and cannot be separated.

Alternatively, Eq. 1.4 can be rearranged to calculate force as a function of Ca^{2+} concentration, but in general nonlinear least mean square algorithms must then be used (see Methods). Fig. 2 shows the force recorded in response to three stimuli applied to a bundle of fibers from the rat soleus muscle, together with the force predicted from different models. The experimental data are the same in all three parts of the figure and the data points have been

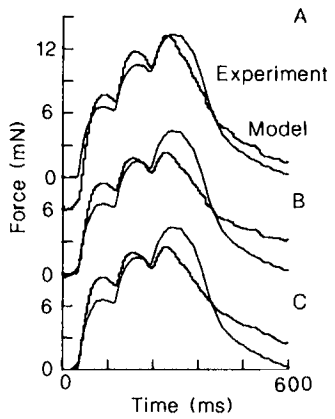

FIGURE 2 The force generated by a bundle of rat soleus muscle fibers is shown as smooth lines (*Experiment*) in the three parts of this figure. The predicted force is shown in the form of bar histograms (*Model*) for three different versions of a model. The model assumes that Ca^{2+} binding is rate-limiting for force production and that binding a single Ca^{2+} can produce force. Parameter values have been increasingly constrained in going from *A* to *B* and *C*. The fit of the model predictions to the experimental data is not very good in any part of the figure, but deteriorates as parameter values become more constrained.

TABLE I
RESIDUAL ERROR AND BEST-FITTING PARAMETERS FOR THE CURVES SHOWN IN THE FIGURES

Fig. 2	ERR/SD	am	b	o					
	%								
A	29	345	7.9	−12.6					
		a	b	o					
B	42	8.1	6.3	−11.5					
C	48	6.8	8	0					
Fig. 3									
A1	40	8.5	8.0						
A2	29	17.7	5.1						
A3	28	23.4	3.6						
B1	16	0.26	1.5						
B2	7	1.0	1.3						
B3	14	1.5	0.97						
C1	60	16.3	13.6						
C2	50	20.2	6.7						
C3	47	24.6	5.1						
		a_1	a_2	b_1	b_2				
A2S	31	50	13.4	4.2	9				
B2S	9	1.5	0.75	0.46	2.25				
C2S	27	9	205	0.2	46				
Fig. 4		f_0	g	K_1	K_2				
A1	33	6.8	7.4	0.77	0.50				
B1	14	3.2	1.6	1.9	5.7				
C1	39	0.06	18.6	1.0	0.25				
		f_0	g_0	g_1	K_1	K_2	T		
A2	9	3.0	2.1	13.5	1.4	0.13	350		
B2	8	0.25	0.45	2.0	1.5	1.0	488		
C2	11	5.0	4.0	58	13.7	0.008	240		
		f_0	f_1	f_2	g_0	g_1	K_1	K_2	T
A3	6	4.0	0.045	0.096	2.1	12.8	5.0	0.1	350
B3	16	0.05	0.12	0.14	0.24	1.2	1.6	0.26	496
C3	13	10	0.31	337	0.85	56	1.1	0.23	240
		a_1	a_2	b_1	b_2	f	g_0	g_1	
A4	26	10	134	12.7	28	36	17	1.0	
B4	14	0.25	3.8	1.2	9.5	75	2.3	0.05	
C4	25	15	982	6.2	76	39	73	0.13	

Fig. 5		f_0	g_0	g_1	K_1	K_2	T
1	9	3.0	3.8	14	1.6	0.13	150
		2.7–3.3	3.4–4.3	13–16	1.4–1.8	0.12–0.14	140–155
2	10	3.0	2.8	14	2.2	0.13	250
		2.7–3.2	2.3–3.1	13–16	2.1–2.5	0.12–0.15	240–255
3	9	3.0	2.1	13.5	1.4	0.13	350
		2.8–3.2	1.8–2.5	12–15	1.3–1.6	0.12–0.14	345–355
10	6	3.0	1.1	14	1.6	0.13	1050
		2.9–3.0	0.9–1.2	13–15	1.6–1.7	0.13–0.14	1,045–1,055
Avg.	8.5	3.0	2.5	13.9	1.7	0.13	

Times (T) are given in milliseconds, dissociation constants (K_1, K_2) in μM, rate constants in s^{-1} or $(\mu Ms)^{-1}$, as appropriate. 95% confidence intervals are listed for each parameter in Fig. 5.

connected to give a smooth curve. The force predicted by Eq. 1.4 is shown in Fig. 2 *A* in the form of a histogram with step changes between each value and has a serrated appearance. The best-fitting parameters in Fig. 1 *A* are $p = 0.023$ μM/mN, $q = 0.0025$ μMs/mN, $r = 2.9$ μM. The corresponding model parameters (b, o, and the product am) are given in Table I for this and all other curves shown in the figures.

The constants m and o are actually constrained by the fact that when x_1 reaches its maximum value of 1, force must approach its maximum value F_{tet}, so

$$F_{tet} = m + o. \tag{1.5}$$

In addition, prior to stimuli being applied, the resting Ca^{2+} concentration will produce a positive, resting, steady-state value (ss) of x_1, leading to a positive resting value of force. In contrast, to optimize the fit in Fig. 2 *A*, a substantially negative, initial value of force resulted (nearly -3 mN). To avoid this, we set

$$F^{ss} = mx_1^{ss} + o, \tag{1.6}$$

where $x_1^{ss} = ac^{ss}/(ac^{ss} + b)$ from Eqs. 1.1 and 1.2. Eqs. 1.5 and 1.6 can be used to eliminate the parameters m and o.

For a given value of n, only the two kinetic parameters (a and b) remain to be determined. The problem of parameter estimation is now a nonlinear one, and each parameter must be varied systematically so as to minimize the mean square deviations of the fitted curve from the experimental data (see Methods). The results are shown in Fig. 2 *B* and the best-fitting values of the parameters are listed in Table I.

Two potential problems are apparent in this model. The predicted fraction of bonds formed at rest is somewhat high. From the best-fitting parameters in Table I, Eq. 1.6 would predict that between 25 and 30% of troponin should have Ca^{2+} bound and thus that over 25% of the maximum number of cross-bridges would be made at rest. Typically, muscle stiffness increases by a factor of 5 or more from rest to tetanic values (Stein and Gordon, 1986), suggesting that <20% of crossbridges are made at rest. The fraction predicted by the model is therefore somewhat high, particularly since some of the resting stiffness may be due to parallel elastic elements. Another potential problem arises from the fact that the values of Ca^{2+} in Fig. 2 are estimated from the light released by aequorin using the method of Allen and Blinks (1979), but there is a Ca^{2+}-independent component of this light, which might affect the estimates of force at low levels of Ca^{2+} (see Methods).

To check the possible effects of these two phenomena, the best-fitting values of a and b can be recalculated, assuming that $m = F_{tet}^{-1}$ and $o = 0$ (Fig. 2 *C*). Not surprisingly, as the model is constrained to have preset values of tetanic tension (Fig. 2 *B*) and offset (Fig. 2 *C*), the fit becomes progressively poorer, although the fit to the data is not particularly good anywhere in Fig. 2. The standard deviation (SD) of the experimentally measured force values from the mean in Fig. 2 was 4.5 mN, whereas the RMS error (ERR) of the force values from the fitted curve was only 1.3 mN or 29% of SD in B of Fig. 2. The residual variance is only $(0.29)^2 = 8.4\%$ of the original variance and a measure corresponding to a linear correlation coefficient would give a value of 0.96 for this reduction in variance. For comparison, the error of the force values from the fitted curve was 1.87 mN in Fig. 2 *A* and 2.17 mN in Fig. 2 *C*, so ERR/SD = 42 and 48%, respectively.

The dissociation constant K_d equals b/a in the simple first order model, and this gives the Ca^{2+} concentration at which half the maximal force level will be generated. The predicted values of K_d are 0.78 μM for Fig. 2 *B* and 1.19 μM for Fig. 2 *C*. These values differ somewhat from the experimental value of 0.6 μM reported by Stephenson and Williams (1981) in skinned rat soleus muscles. Stephenson and Williams (1981) also found that the steady-state data were best fitted when 2 or sometimes 3 Ca^{2+} had to be bound to troponin to produce force. Fig. 3 *A* shows the same force data as in Fig. 2, fitted under the assumption that $n = 2$ and $n = 3$. The fits are improved somewhat with ERR/SD = 29% ($n = 2$) and 28% ($n = 3$). These percentages are comparable to the best fits found in Fig. 2. Fewer free parameters are available here than in Fig. 2, *A* and *B*, since the offset is now fixed at zero and the maximum is fixed at the measured tetanic value.

From Eqs. 1.1 and 1.2 the steady-state value of Ca^{2+} is

$$c^{ss} = K_d x_1^{ss}/(1 - x_1^{ss}), \tag{1.7}$$

where $x_1^{ss} = (F^{ss}/F_{tet})^{1/n}$ and $K_d = b/a$. For the model of

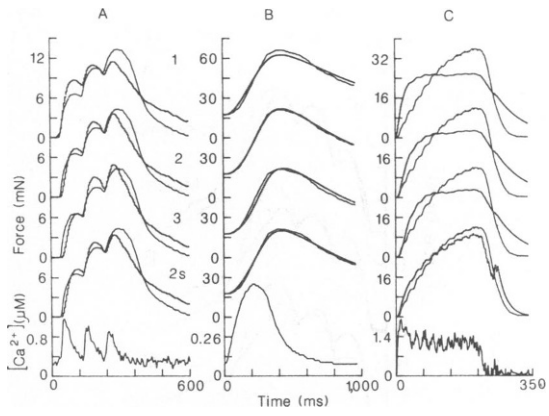

FIGURE 3 Further predictions for the force generated by models in which Ca^{2+} binding is rate-limiting for force production in (*A*) rat, (*B*) barnacle, and (*C*) frog skeletal muscle fibers. From top to bottom, it was assumed that 1 (as in Fig. 1), 2, or 3 Ca^{2+} ions must bind independently to troponin for force generation. In the fourth row (2*s*), it was assumed that two Ca^{2+} ions must bind to troponin for force generation, but that binding occurs sequentially at the two sites, rather than independently. The bottom row shows the observed Ca^{2+} transients used in these predictions. The closest fit is given by (*A*) 3, (*B*) 2, and (*C*) 2s, but the effects of different binding numbers or degrees of cooperativity are small for the most part. Data in *A* are the same as that in Fig. 2.

Fig. 3 with $n = 2$, $a = 17.7$ $(\mu Ms)^{-1}$, and $b = 5.1$ s^{-1} so $K_d = 0.288$ μM and $c^{ss} = 0.69$ μM for half-maximal force production. The corresponding values for $n = 3$ give $c^{ss} = 0.59$ μM, which is close to the measured value of 0.60 μM given by Stephenson and Williams (1981). Thus, although the fit is not greatly improved over Fig. 2, there are fewer free parameters and the best-fitting values of the parameters are more realistic.

2. Contraction Limited by Sequential Binding of Calcium

Stephenson and Williams (1981) found better agreement to their data by assuming sequential, rather than independent binding of Ca^{2+} to troponin. Let x_0, x_1, and x_2 be troponin molecules with 0, 1, or 2 Ca^{2+} ions bound according to the reaction scheme shown in Fig. 1 *B*, where there are now two distinct forward (a_1 and a_2) and backward (b_1 and b_2) rate constants. The differential equations are now

$$dx_0/dt = -a_1cx_0 + b_1x_1 \tag{2.1}$$

and

$$dx_2/dt = a_2cx_1 - b_2x_2 \tag{2.2}$$

with the condition that

$$x_0 + x_1 + x_2 = 1. \tag{2.3}$$

From Eqs. 2.1–2.3 the steady-state value is

$$x_2^{ss} = c^2/(c^2 + cK_2 + K_1K_2), \tag{2.4}$$

where $K_1 = b_1/a_1$ and $K_2 = b_2/a_2$ are the dissociation constants of the two stages of the reaction. It can easily be shown that if $K_2 < 4\ K_1$, there is positive cooperativity in the binding of Ca^{2+} to troponin. Cooperativity between Ca^{2+} binding and actomyosin binding has been studied experimentally (e.g., Bremel and Weber, 1972) and modeled extensively by Hill et al. (1980, 1981). Although their models contain too many free parameters to be used here, the predicted degree of cooperativity (see dotted line in Fig. 3 of Hill et al., 1980) is within the range that can be fitted by our simpler model (see also Fig. 7).

We will also assume that x_2 is the only state that allows force production ($x_2 = F/F_{tet}$). Although there are now four rate constants to be determined rather than two, the same nonlinear least mean squares techniques can be used as in the previous section and the results are shown as row 2s in Fig. 3 for comparison with the other models. ERR/SD = 31% so adding two extra parameters did not improve the fit to the data.

The only study to our knowledge that claims a good prediction of force from measured free Ca^{2+} transients, under the assumption that the sequential binding of Ca^{2+} to troponin is rate limiting, was that of Ashley and Moisescu (1972). In their experiments, small amounts of force (~6.5% of tetanic value) were produced by single voltage clamp pulses to barnacle muscle fibers. Fig. 3 *B* compares the results for these fibers from the model of Section 1 with $n = 1, 2$, and 3 and the sequential model (2s) developed in this section. The fits of all the models are substantially better than for the rat muscle with ERR/SD = 16% (n = 1), 7% ($n = 2$), 14% ($n = 3$), and 9% ($n = 2$s). Again, the sequential model does not provide an improved fit, despite the extra free parameters. Furthermore, the relatively small range of data available does not allow one to distinguish adequately between the various models. Finally, Fig. 3 *C* shows the force predicted by the four models for a third data set in which a short tetanus was applied to a single frog muscle fiber. For these frog data only the sequential model (2s) seems to give an adequate fit.

3. Contractions Limited by Acto-Myosin Cross-Bridge Formation

Let us now consider the opposite assumption, namely that Ca^{2+} kinetics are rapid and that contraction is limited by acto-myosin bond formation. Over the years many models of this process have been suggested. We begin by considering the simplest model (Fig. 1 *C*) in which the cross-bridge exists in either a detached state (y_0) or a force-generating one (y_1), and f and g are the rate constants for attachment and detachment, respectively, following Huxley (1957). Somewhat more complex models will be considered later (Sections 4–6), but for this simple model

$$dy_1/dt = fy_0 - gy_1 \tag{3.1}$$

and

$$y_0 + y_1 = 1. \tag{3.2}$$

Huxley (1957) considered the effect of position and velocity on the movement, but assumed that the muscle was fully activated (all troponin molecules had Ca^{2+} bound) and was able to generate tetanic levels of force. The attachment rate constant f should be proportional to the fraction of troponin which is activated. If Ca^{2+} kinetics are sufficiently fast, at least when actin and myosin are detached, the equilibrium relation can be used for the models of Section 1, namely

$$f = f_0[c/(c + K_d)]^n, \tag{3.3}$$

where f_0 is the maximum attachment rate constant and the dissociation constant $K_d = b/a$ as before. The detachment rate is really a composite of the rate at which Ca^{2+} unbinds and the cross-bridges detach, plus the rate at which cross-bridges detach with Ca^{2+} still attached. Examples where neither Ca^{2+} kinetics nor crossbridge kinetics can be ignored and interactions between the two must be considered explicitly, will be dealt with in Section 6. Similarly,

for the sequential model of Section 2,

$$f = f_0[c^2/(c^2 + cK_2 + K_1K_2)] \tag{3.4}$$

and K_1 and K_2 are the two dissociation constants, as defined in relation to Eq. 2.4.

The steady-state value of y_1 from Eqs. 3.1 and 3.2 is

$$y_1^{ss} = f/(f + g) \tag{3.5}$$

and for large values of c, Eqs. 3.3 and 3.4 both give $f = f_0$. Force will reach its tetanic value F_{tet} under these conditions, so

$$F/F_{tet} = y_1(f_0 + g)/f_0. \tag{3.6}$$

Eq. 3.6 makes the assumption that force is proportional to the number of bonds made (y_1). Clearly, this will not be true if the bonds are stretched or the rate constants are position-dependent, as Huxley (1957) considered, but this simplifying assumption is adequate for the isometric conditions considered here. For a given value of n in Eq. 3.3, there are now 3 pm to be determined (f_0, g, and K), whereas with Eq. 3.4 there are 4 pm (f_0, g, K_1, and K_2).

The same data sets as in Fig. 3 have been fitted with these models using Eq. 3.4 and the results are shown in row *1* of Fig. 4. The results should be compared with row 2s in Fig. 3, because the sequential model for Ca^{2+} binding was used. The fits are actually somewhat worse (see Table I) and there are obvious disparities between the measured values and the fitted curves. Similar results were obtained with different values of n from Eq. 3.3, but only the results from Eq. 3.4 (sequential binding of Ca^{2+}) are shown in this and subsequent figures for simplicity.

An interesting ratio is $f_0/(f_0 + g)$, which is the fraction of bonds made when Ca^{2+} ions are bound to all possible troponin sites and force reaches its tetanic level. With the best-fitting values of f_0 and g, the model predicts that 48% of the crossbridges will be made for the rat muscle (row 1 of Fig. 4 *A*) and 67% for the barnacle muscle (row *1* of Fig. 4 *B*). For these two muscles, the predictions are in agreement with experimental estimates, although these estimates vary fairly widely when obtained by different techniques: x-ray diffraction (45–58%, Haselgrove and Huxley, 1973; 80–89%, Matsubara et al., 1975), stiffness measurements (75 ± 7%, Goldman and Simmons, 1977); EPR spectroscopy (20%, Cooke et al., 1984). For the frog data, however (row 1 in Fig. 4 *C*), totally unrealistic predictions are obtained (<0.3% of crossbridges attached during a tetanus). We will now consider how such large discrepancies can be eliminated.

4. Time-dependent Detachment Rate Constants

The problem that can be clearly seen in Figs. 2–4 is that curves that fit the rising phase are too slow for the relaxation phase and curves that fit the relaxation phase

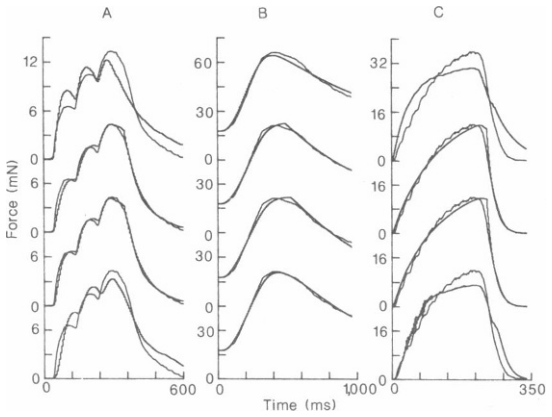

FIGURE 4 The same data as in Fig. 3 are fitted with models in which cross-bridge kinetics are rate-limiting (rows *1*, *2*, and *3*) or in which both Ca^{2+} kinetics and cross-bridge kinetics contribute (row *4*). Either a two-state (rows *1*, *2*, and *4*) or a three-state (row *3*) cross-bridge kinetic model has been used, and a time-dependent detachment rate constant was (rows *2*, *3*) or was not (rows *1*, *4*) allowed. Ca^{2+} binding followed first-order (row *4*) or second-order, sequential kinetics (rows *1*, *2*, and *3*). The simplest model which gives a good fit to all the data is that for row *2*, which is developed in Section 4 and elaborated in Section 7 of Results.

are too fast for the rising phase. Simple first- and second-order systems such as considered in the previous sections are constrained in that the rate constant for the rise of force must be greater than or equal to the rate constant for the falling phase. However, if exponentials are fitted to a partially fused tetanic contraction such as shown in Figs. 3 and 4, the rising rate constant is actually less than the falling rate constant. The values are 8.9 s^{-1} and 45 s^{-1}, respectively, for the frog tetanus in Fig. 3 *C* (see also Stein et al., 1982 for values in mammalian muscles). The rising rate constant was increased somewhat in a fully fused tetanus, but still remained well below the value of 45 s^{-1} for the falling rate constant.

Clearly, some mechanism must be present that increases the dissociation of bonds on the falling phase of the contraction. Possible mechanisms will be considered in the Discussion, but let us simply assume for the moment that the formation of bonds and the turnover are initially slow, but at some point in time the detachment rate increases to a high value. For the two-state model shown in Fig. 1 *D*, we have

$$g = \begin{matrix} g_0 & t < T \\ g_1 & t \geq T \end{matrix} \tag{4.1}$$

where T is an unknown constant. With F_{tet} specified there are still 6 pm that must be determined for the relation between Ca^{2+} and force: f_0, K_1, K_2, g_0, g_1, and T.

The results of fitting the same data sets with a time-dependent rate constant for breaking crossbridges are shown in row *2* of Fig. 4. The deviation of the predictions from the data is now greatly reduced. For example, ERR/SD for the rat muscle is now reduced to only 9%,

compared with between 30 and 40% in previous figures. Similarly, ERR/SD in the frog muscle is only 11%, compared with between 27 and 60% in previous figures. The improvements are not as dramatic for the barnacle, since the fits were already very good in Fig. 3 *B*, but there is a further reduction of ~5% in ERR/SD between rows 1 and 2 of Fig. 4 *B*. Finally, the predictions for the fraction of cross-bridges that are made in a tetanic state range from 35 to 60% for all three data sets, which is within the range of experimental estimates described above.

One residual problem is that the sharp transition between one rate constant and the other at time T produces an abrupt change of slope in force, a change that is not observed experimentally. In addition, for the three pulses in Fig. 4 *A* the downturn in force after each pulse is not fitted precisely. Clearly, a smooth transition that begins whenever force begins to decline would be preferable to a single, sharp transition.

5. Three-state Cross-bridge Models

The two-state model considered above is an extreme oversimplification. More recent experimental data have suggested models containing three or more mechanical states (Huxley and Simmons, 1971; Goldman et al., 1984), and the number of biochemical states is considerably larger (Hibberd and Trentham, 1986). In this section we will use the three-state model suggested by Goldman et al. (1984; see also Bobet, 1986), although with somewhat different notation for consistency with previous sections. In addition to a free or unattached state (y_0) and an attached, active force-producing state (y_1), Goldman et al. (1984) included a rigor state, which we will call y_2. In this state, bonds are attached and contribute to muscle stiffness, but produce less force. If we denote the new forward rate constants by f_1 and f_2, the model is given by the diagram of Fig. 1 *E*. Goldman et al. (1984) also required one back rate constant from the active to the detached state to fit their data. We have denoted this rate constant by g and allowed the switching to occur either in g (from g_0 to g_1) or in the transition from the active to the rigor state (from f_{10} to f_{11}). Yet another interpretation which is consistent with much recent experimental data (Eisenberg and Hill, 1985; Brenner and Eisenberg, 1987) is to assume that y_0 is a composite of a free and a weakly attached state which are in rapid equilibrium. Then, f is the transition from a weakly to a strongly attached state. In any case, there are now two differential equations

$$dy_1/dt = fy_0 - (f_1 + g)y_1 \tag{5.1}$$

$$dy_2/dt = f_1y_1 - f_2y_2 \tag{5.2}$$

plus the condition that

$$y_0 + y_1 + y_2 = 1. \tag{5.3}$$

In the steady state ($dy_1/dt = dy_2/dt = 0$), Eqs 5.1–5.3 can be solved to give

$$y_1^{ss} = ff_2/D \tag{5.4}$$

$$y_2^{ss} = ff_1/D \tag{5.5}$$

where $D = f_2(f + f_1 + g) + ff_1$. The rate of cross-bridge cycling is given by

$$f_1y_1 = ff_1f_2/D \tag{5.6}$$

and its inverse is the cycle time T_c

$$T_c = f^{-1} + f_1^{-1} + f_2^{-1} + g/(ff_1). \tag{5.7}$$

As in the previous section we will assume that Ca^{2+} kinetics are rapid compared to the cross-bridge cycling and that they are given by Eq. 3.4. When Ca^{2+} levels are high, $f = f_0$, as before. The level of force generated will be

$$F = c_1y_1 + c_2y_2, \tag{5.8}$$

where c_1 and c_2 are constants. The tetanic level (F_{tet}) will be

$$F_{tet} = f_0(c_1f_2 + c_2f_1)/D_0, \tag{5.9}$$

where $D_0 = f_2(f_0 + f_1 + g) + f_0f_1$. As before, we will be interested in the ratio

$$F/F_{tet} = [(y_1 + ry_2)D_0]/[(f_2 + rf_1)f_0], \tag{5.10}$$

where $r = c_2/c_1$ is the force production of the rigor state relative to the active state ($0 < r < 1$).

The predictions of this model are shown in row *3* of Fig. 4. Despite the extra kinetic constants (f_1 and f_2), the fits are only marginally improved over those of the two-state model (row *2* in Fig. 4). The particular curves shown assumed that $r = 0$ (the bonds in the rigor state generated no force). However, other values of r made very little difference to the goodness of fit. In the data shown the switching occurred in the value of g, but there was little difference in the fit if the switching occurred in f_1. The best-fitting parameters for the rat soleus muscle predicted a cycle rate from Eq. 5.6 of 0.022 s^{-1} if g was switched and 1.42 s^{-1} if f_1 was switched, whereas the experimentally measured rate is close to 1 s^{-1} (Stein et al., 1982). For comparison the predicted cycle rate was 1.36 s^{-1} for the two-state model in row *2* of Fig. 4. Thus, adding the extra complexity of a three-state model seems unwarranted for the present purposes.

6. Do Both Ca^{2+} and Cross-Bridge Kinetics Contribute to Force Generation?

Until this point we have assumed that either Ca^{2+} kinetics or crossbridge kinetics are rate-limiting. However, it is certainly possible that both limit force production and a model which incorporates that possibility is shown in Fig.

1 F. The properties of each state are indicated by the words nearest that state: y_0 = fraction of crossbridges with no Ca^{2+} bound and producing no force, y_1 = fraction with Ca^{2+} bound but not generating force, y_2 = fraction with Ca^{2+} bound and generating force, and y_3 = fraction with no Ca^{2+} bound, but still generating force. Once this force is gone, it cannot be generated, except by repeating the cycle, so the transition from y_3 to y_0 is shown as an irreversible reaction.

There are now three differential equations

$$dy_1/dt = a_1cy_0 - (f + b_1)y_1 + g_1y_2 \quad (6.1)$$

$$dy_2/dt = fy_1 - (g_1 + b_2)y_2 + a_2cy_3 \quad (6.2)$$

$$dy_3/dt = b_2y_2 - (g_0 + a_2c)y_3 \quad (6.3)$$

with the condition that

$$y_0 + y_1 + y_2 + y_3 = 1. \quad (6.4)$$

In the steady state $dy_1/dt = dy_2/dt = dy_3/dt = 0$ and Eqs. 6.1–6.4 can be solved analytically. The solutions are

$$y_1^{ss} = a_1c[g_1(g_0 + a_2c) + b_2g_0]/D \quad (6.5)$$

$$y_2^{ss} = a_1cf(g_0 + a_2c)/D \quad (6.6)$$

$$y_3^{ss} = a_1cfb_2/D, \quad (6.7)$$

where $D = (a_1c + b_1)\ [g_1(g_0 + a_2c) + b_2g_0] + a_1cf(g_0 + a_2c + b_2) + fb_2g_0$. Note that if $c = 0$, $y_1^{ss} = y_2^{ss} = y_3^{ss} = 0$, so $y_0^{ss} = 1$. If $c = \infty$, then $y_0 = y_3 = 0$, $y_1 = g_1/(f + g_1)$, $y_2 = f/(f + g_1)$, and

$$F = F_{tet}\,(y_2 + y_3)\,(f + g_1)/f. \quad (6.8)$$

A priori, this model seems to share some features of the model of Section 4, because there are two distinct detachment rate constants g_0 and g_1. Furthermore, one may be most important on the rising phase when Ca^{2+} levels are high and the other most important on the falling phase when Ca^{2+} levels are low. The best-fitting values are given in row *4* of Fig. 4. Despite the large number of parameters and the analogy to the models with time-dependent rate constants, the fits are only slightly better than those of row *1* and not nearly as good as those of rows *2* and *3*. Clearly, a large number of parameters is no guarantee of success in fitting the experimental data.

7. Further Predictions for the Model of Section 4 with Time-dependent Rate Constants

Good fits were obtained with a model that was developed in Section 4. The predictions of this model which had relatively few free parameters will be examined further in this last section of Results. In row *2* of Fig. 4 *A*, the response of a small bundle of rat soleus muscle fibers to three stimuli was shown. The response of the same bundle to (*A*) 1, (*B*) 2, and (*C*) 10 stimuli is shown in Fig. 5. Each data set was fitted independently and the residual errors were <10% in each part of the figure.

The goodness of the fit is quite remarkable if one considers the complex pattern of nonlinear summation which is occurring in these data. Fig. 6 *A* illustrates this nonlinear summation for Ca^{2+} and force. The Ca^{2+} trace shows the response to 10 stimuli and, as was already clear from Fig. 2, substantially less Ca^{2+} is being released by each successive stimulus. In contrast Fig. 6 *B* shows the additional force contributed by the first (twitch), second, third, and tenth stimulus. All have been lined up with respect to the time of stimulation, and the contributions would be identical if the force produced by each stimulus summed linearly. Instead, a complex series of amplitude and time-dependent nonlinearities is observed, as previously reported (Stein and Parmiggiani, 1981; Stein and Gordon, 1986).

The pattern of nonlinear summation predicted by the model is shown in Fig. 6 *C*. The model was run on the data for 1, 2, 3, 9, and 10 pulses, and the predicted force obtained for each data set was analyzed in an identical manner to that used to obtain Fig. 6 *B*. Clearly, the model's predictions agree very closely with the experimental data, although the effect of the discontinuity in the detachment rate constant does lead to some difference in time course. The important point here is that the good fit to this complex pattern of nonlinear summation followed from the model without any special assumptions.

Because each data set was fitted independently in Fig. 5, it is of interest to consider any systematic changes in the best-fitting parameters as the period of stimulation was increased. The parameter values are given in Table I and most parameters are independent of the stimulus number. One obvious exception was T, the time at which the detachment rate increased from its low initial value g_0 to a higher value g_1. As might be expected, T increased with the duration of the contraction. The other exception was the

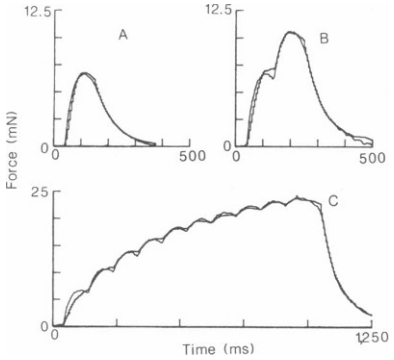

FIGURE 5 Observed and predicted force (using the model of Fig. 1 *D*) for the same rat soleus muscle shown in Figs. 2–4. Here (*A*) 1, (*B*) 2, or (*C*) 10 supramaximal, electrical stimuli were applied at an interval of 100 ms. A good fit is observed in all parts of the figure.

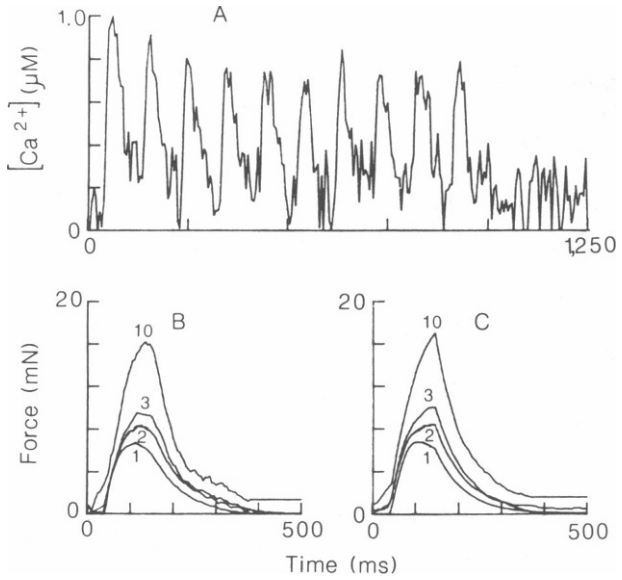

FIGURE 6 The time course of free Ca^{2+} in response to 10 stimuli at 100-ms intervals (*A*) shows a decrease in free Ca^{2+} produced by successive stimuli. The extra force contributed by the first, second, third, and tenth stimulus in a train as measured experimentally (*B*) and as predicted by the model of Fig. 1 *D* (*C*) both show that the extra force contributed by additional stimuli increases despite the decreasing Ca^{2+} input.

detachment rate constant g_0, which decreased systematically as the number of stimuli increased. The reasons for this decrease will be considered in the Discussion.

Finally, the parameters determined here can be used to predict the steady-state curve of force vs. Ca^{2+}, which has been measured for skinned fibers from this same muscle by Stephenson and Williams (1981). The prediction is shown in Fig. 7 and has the well-known sigmoidal shape. In the model of Eq. 3.4, half-maximal force will be obtained at a Ca^{2+} concentration of 0.35 μM (pCa = 6.46), a value close to the average value obtained by Stephenson and Williams (1981) of 6.22. Furthermore, the force in the model goes from 10 to 90% of its tetanic value over a pCa range of 1.07, a range similar to the average value of 0.95 measured by Stephenson and Williams (1981). The agreement is satisfactory considering the differences in experimental techniques (skinned vs. intact fibers, bath application vs. release from the sarcoplasmic reticulum, temperatures of 22°–25°C vs. 20°C). The sequential, second-order model has a steep slope which gives a better fit to the experimental data than a model with independent binding of either 2 or 3 Ca^{2+} ions. The steepness of the slope may also arise from changes in Ca^{2+} affinity (Potter, 1988), but the sequential second-order model is adequate until more details of the affinity changes become available.

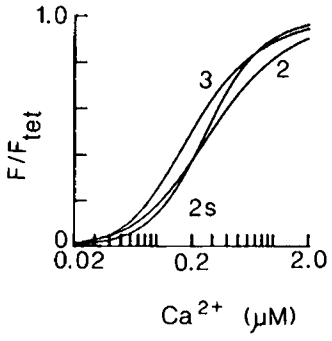

FIGURE 7 Steady-state relation predicted for the model of Fig. 1 *D* between Ca^{2+} concentration (plotted on a logarithmic scale) and force (normalized to its tetanic level). The predicted values for the sequential model (*2s*) agree better with the experimental observation of Stephenson and Williams (1981) than the models with 2 or 3 Ca^{2+} binding independently to troponin.

DISCUSSION

The models considered here contain only two or three states for the Ca^{2+} kinetics and the crossbridge kinetics, whereas biochemical models of the crossbridge kinetics alone may contain up to 14 states (Hibberd and Trentham, 1986). However, many of these states do not contribute significantly to force generation and would not be detected from the data analyzed. As was evident in several sections of the Results, adding more states to the models may not significantly improve the fits obtained. In essence, by using models with relatively few states, we are trying to determine which of the many biochemical reactions observed in a test tube is (are) rate-limiting for force generation under physiological conditions.

Ca^{2+} Kinetics

Models of Ca^{2+} kinetics often include the many Ca^{2+} binding proteins contained in muscle (e.g., Cannell and Allen, 1984). The binding to these proteins will certainly modify the time course of the free Ca^{2+} concentration, but we are not trying to model this time course. Rather, we have taken it as a starting point and asked how this free Ca^{2+} will interact with troponin to produce force.

Cannell and Allen (1984) also tried to take into account inhomogeneities in Ca^{2+} concentration by including equations for the diffusion of free Ca^{2+} from its release sites to its binding sites. These inhomogeneities are of concern here because the light signal from aequorin will be very sensitive to any hot spots of Ca^{2+}, since light varies as a power of Ca^{2+} concentration. However, all studies to date have found that the decay of Ca^{2+} can be well fitted over most of its time course by a single exponential (e.g., Cannell, 1986; Fryer and Neering, 1986). If the process were diffusion-limited and the aequorin signals were badly distorted by inhomogeneities, this would not be expected. Thus, significant distortions due to diffusion are probably restricted to the very brief rising phase of the Ca^{2+} transient, if they are present at all, and are unlikely to affect our predictions of the much slower time course of force generation in any major way.

One of the interesting results of our analysis was that none of the standard kinetic models for Ca^{2+} binding to troponin adequately predicted the time course of force

production except perhaps for the barnacle muscle. However, the limited range of the barnacle data precluded a very rigorous test. More complex models have been suggested (Hill et al., 1980, 1981) to account for the complexity of Ca^{2+} and actomyosin binding first described by Bremel and Weber (1972). Recently, Potter (1988) found that crossbridge cycling can increase the affinity of Ca^{2+} for troponin by a factor of ten, and it is possible that a more complex model incorporating affinity changes would provide a better fit. On the other hand, recent evidence by Kress et al. (1986) indicates that structural changes, probably corresponding to Ca^{2+}-induced tropomyosin movement, take place long before force is generated in frog muscles. Thus, Ca^{2+} binding to troponin is probably not rate-limiting for force production, as will be considered further below (see Crossbridge Rates). However, standard kinetic models of crossbridge cycling did no better in predicting force than the models of Ca^{2+} binding, and this point needs further discussion.

Rate Constants for Force Production

In retrospect, the lack of agreement between predictions from standard models of Ca^{2+} kinetics and cross-bridge kinetics and the experimental data could have been foreseen. For example, the exponential rate of rise of force at the beginning of a tetanus for most muscles is slower than the exponential decay of force at the end of a tetanus (e.g., Stein et al., 1982). For the two-state model of Fig. 1 *A*, there is only a single rate constant, which is given by the sum $(ac + b)$. This rate constant can vary if c varies, but it would be higher for the rising phase of force generation, when the Ca^{2+} concentration is high, than for the falling phase when it is low, just the opposite of what is found experimentally. A similar result will apply to the two-state crossbridge model of Fig. 1 *C*, if the parameter f is higher in the presence of Ca^{2+} on the rising phase of force production than in the relative absence of Ca^{2+} on the falling phase.

A three-state model for Ca^{2+} kinetics (Fig. 1 *B*) or crossbridge kinetics (Fig. 1 *E*) can have two independent rate constants, but the response to a brief input will always be such that the decay phase will be determined by the slower of the two rate constants, again opposite to what is found experimentally. This basic mathematical fact has hindered attempts to fit models containing two rate constants to muscle force for years (Jewell and Wilkie, 1958; Mannard and Stein, 1973). The problem can be overcome formally, if the rate constant for crossbridge detachment is switched during the falling phase of force generation to a much higher value (Fig. 1 *D*). The residual errors then decrease dramatically (Table I, Fig. 4), a consistent set of parameters is obtained for data arising from different numbers of stimuli (Table I, Fig. 5), and the complex pattern of nonlinear summation is fitted accurately (Fig. 6).

What Is Switched?

Huxley (1957) included a step increase in his detachment rate constant when a bond moved from one side of its equilibrium position (where it generated force) to the other side (where it absorbed force). Thus, this switching function can be viewed as a normal part of the crossbridge cycle. The switching of detachment rates will be accentuated by the dispersion of sarcomeres first described by Cleworth and Edman (1972). For example, during relaxation some sarcomeres which have more attached crossbridges will shorten at the expense of others which have fewer. Crossbridges in the sarcomeres that are shortening will move into Huxley's region where the detachment rate is high and sarcomeres that are being lengthened may be stretched enough that the elastic limit of the crossbridges is exceeded and the bonds are broken (Hill, 1968).

Thus, the breakage of bonds would be particularly high during relaxation, as observed for the parameter g_1. Furthermore, during the rising phase of a twitch, when there is also partial activation of sarcomeres and some shortening may be occurring against the muscle's series elasticity, a relatively high rate of breakage would be expected. This rate would decline when more stimuli are added to the train, activation becomes more complete, and the series elasticity is well stretched. This trend was in fact observed for the parameter g_0 in Table II.

The above analysis explains the changes in detachment rate qualitatively in terms of known crossbridge mechanisms, but it remains to consider what determines the time T at which the rate switches and the exact value of g_1. Recent work by Cannell (1986) indicates that the relaxation phase, which he calls period 3, is associated with a level of Ca^{2+} (between 0.5 and 1 μM), which is low, but still considerably elevated above resting values (~0.1 μM). These low levels are not well resolved in our data, so we cannot be certain whether the time T always corresponds to a particular free Ca^{2+} concentration or one of its complexes with troponin (El-Saleh et al., 1986). Either of these possibilities would be consistent with Cannell's (1986) data.

Table II summarizes published data for the exponential decay rates of Ca^{2+} concentration and force in various muscles. The decay rate of Ca^{2+} is equal to or greater than that of force in all the muscles examined. Where the decay rates are similar (fast-twitch muscles), one might postulate that the decay of Ca^{2+} directly leads to the detachment of cross-bridges and the decay of force. Where the rate of Ca^{2+} decay is faster, one could assume that intervening processes, such as the release of Ca^{2+} by troponin or the detachment of cross-bridges, slow the force decay further. However, the Ca^{2+} decay rate may slow during the period when force decays rapidly both in frog (Cannell, 1986) and barnacle muscles (Ashley and Lignon, 1981), so the Ca^{2+} and force decay rates may be closer than indicated in Table II.

TABLE II
COMPARISON OF FORCE AND CALCIUM DECAY RATES

Muscle	Force	Calcium	Temperature	Reference
	s^{-1}	s^{-1}	°C	
Rat soleus	8.5	16	20	Fryer and Neering (1986)
	3.9		20	Stein et al. (1982)
		10*	25	Eusebi et al. (1980)
Rat EDL	25	26	20	Fryer and Neering (1986)
	27		20	Stein et al. (1982)
		25*	25	Eusebi et al. (1980)
Frog TA	49	63	20	This study
Barnacle	4.2	7.7*	10	Duchateau and Hainaut (1986)

*Calcium decay rates were estimated as the 2.5th root of the decays in aequorin luminescence reported in the studies indicated.

Our working hypothesis is that free Ca^{2+} concentration decays rapidly as it is taken up by the sarcoplasmic reticulum and/or bound to Ca^{2+} binding proteins such as parvalbumin in muscle. Force decays slowly until the Ca^{2+} levels approach values near the dissociation constant K_d for Ca^{2+} coming off troponin. Below this level the decay of the free Ca^{2+} concentration may proceed more slowly as the Ca^{2+} coming off troponin replaces some of the Ca^{2+} being pumped out. In addition, while the detachment of cross-bridges is much faster than previously, it is not instantaneous and force may decay more slowly than Ca^{2+} concentration, particularly in slow twitch muscles.

Note that we are not assuming that the rate g depends directly on Ca^{2+} concentration in the way that the rate f does, but rather that low Ca^{2+} levels are a prerequisite for the rapid decay of force. This hypothesis can account for the data summarized in Table II. In some cases, Ca^{2+} decay is relatively slow and force decay will follow roughly in parallel at different temperatures (Stein et al., 1982; Fryer and Neering, 1986) or states of fatigue (Dawson et al., 1980). However, discrepancies between Ca^{2+} and force decay rates do also occur at some temperatures (Fryer and Neering, 1986) and at some muscle lengths (Blinks et al., 1978), indicating that the decay of force is not directly linked to the free Ca^{2+} level.

Crossbridge Rates

Even though we have formally referred to the rate constant which increases during the relaxation phase as the detachment rate constant in our simplified version of Huxley's two-state model, the appropriate rate constant is probably at least one stage back from the actual detachment. Studies using a variety of techniques (Kawai and Brandt, 1980; Goldman et al., 1984; Calancie and Stein, 1987) agree that the detachment of bonds from the rigor state is very fast (values between 100 and 1,000 s^{-1} have been reported). However, the transition from a force-producing state to the rigor state is much slower, and it is this step that may be increased dramatically during the relaxation phase.

Another point that merits discussion here is whether the rise of force is limited by a process that strictly corresponds to the attachment rate constant, the parameter f in Huxley's (1957) model, assuming that Ca^{2+} binding is so fast that it is essentially at equilibrium, or whether the rise of force also depends importantly on Ca^{2+} kinetics. If Ca^{2+} kinetics affected the development of force in a major way, then the rate of rise of a tetanus from rest, when Ca^{2+} is first binding to troponin, would be much slower than the rate of rise of force after a quick release of sufficient magnitude that crossbridges are broken and force transiently returns to the resting level. In fact, the rate constants are normally very similar, for the mammalian muscles considered here (Stein, R. B., and T. Gordon, unpublished observations), although they may differ in muscles bathed in D_2O (Cecchi et al., 1981). Some difference in the rate of force generation has recently been observed between flash photolysis experiments that rapidly release Ca^{2+} and those that rapidly release ATP to skinned muscle fibers (Ashley et al., 1987), although activation of troponin seems to occur well before force generation in intact muscle fibers (Kress et al., 1986). Finally, Calancie and Stein (1987) were able to measure a rate constant for force production in response to small stretches and releases during the plateau of a tetanus (when Ca^{2+} ions remain attached to virtually all troponin molecules) that agreed closely with the rate of rise of force at the start of a tetanus in magnitude and temperature dependence for fast twitch muscles.

Thus, the rate constant for force production appears to be due to crossbridge events, although its value may be influenced by Ca^{2+} kinetics under some circumstances. In terms of current models of muscle (Eisenberg and Hill, 1985), this rate constant f may not apply to the actual attachment of cross-bridges, since formation of weak bonds may occur rapidly. Rather, it is more likely that the rate constant f corresponds to a conversion from weak bonds to strong bonds that can generate substantial levels of force.

In conclusion, although we began by considering quite general models for Ca^{2+} and cross-bridge kinetics to determine the simplest model that accurately fitted the data from a variety of muscles by purely statistical criteria, the analysis has led to a specific model. Finally, the parameters of this model can be related to particular events known to occur in muscle in a way that suggests testable hypotheses about the factors that limit the rate of rise and fall of force under physiological conditions in intact muscle fibers.

This research was supported in part by grants from the Muscular Dystrophy Association of Canada (to R. B. Stein) and the Natural Sciences and Engineering Research Council (to M. N. Oguztöreli). J.

Bobet is a post-doctoral fellow of the Alberta Heritage Foundation for Medical Research.

We thank Dr. I. Neering for support in obtaining the data from rat muscle and Dr. J. Blinks and Mr. N. Lee for assistance in obtaining the data from frog muscle. Drs. C. Kay, T. Gordon, and B. Calancie provided helpful comments on the manuscript.

Received for publication 17 August 1987 and in final form 31 May 1988.

REFERENCES

Allen, D. G., and J. R. Blinks. 1979. The interpretation of light signals from aequorin-injected skeletal and cardiac cells: a new method of calibration. *In* Detection and Measurement of Free Ca^{2+} in Cells. C. C. Ashley and A. K. Campbell, editors. Elsevier/North Holland Press, Amsterdam. 159–174.

Ashley, C. C. 1978. Calcium ion regulation in barnacle muscle fibers and its relation to force development. *Ann NY Acad. Sci.* 307:308–329.

Ashley, C. C., and D. G. Moisescu. 1972. Model for the action of calcium in muscle. *Nature New Biol.* 237:208–211.

Ashley, C. C., and J. Lignon. 1982. Aequorin responses during relaxation of tension of single muscle fibres stimulated by voltage clamp. *J. Physiol. (Lond.).* 318:10–11.

Ashley, C. C., R. J. Barsotti, M. A. Ferenczi, T. J. Lea, and I. P. Mulligan. 1987. Fast activation of skinned muscle fibres from the frog by photolysis of caged-calcium. *J. Physiol. (Lond.).* 394:24p.

Blinks, J. R., R. Rüdel, and S. R. Taylor. 1978. Calcium transients in isolated amphibian skeletal muscle fibres: detection with aequorin. *J. Physiol. (Lond.).* 277:291–323.

Blinks, J. R., W. G. Wier, P. Hess, and F. G. Prendergast. 1982. Measurement of Ca^{2+} concentrations in living cells. *Prog. Biophys. Mol. Biol.* 40:1–114.

Bobet, J. 1986. A model of the motor unit and its implications for the prediction of muscle force during voluntary movement. Ph.D. Thesis, Kinesiology Department, University of Waterloo, Ontario, Canada.

Bremel, R. D., and A. Weber. 1972. Cooperation within the actin filament in vertebrate skeletal muscle. *Nature New Biol.* 238:97–101.

Brenner, B., and E. Eisenberg. 1987. The mechanism of muscle contraction. Biochemical, mechanical, and structural approaches to elucidate cross-bridge action in muscle. *Basic Res. Cardiol.* 82(Suppl. 2):3–16.

Calancie, B., and R. B. Stein. 1987. Measurement of rate constants for the contractile cycle of intact mammalian muscle fibers. *Biophys. J.* 51:149–159.

Cannell, M. B. 1986. Effect of tetanus duration on the free calcium during the relaxation of frog skeletal muscle fibres. *J. Physiol. (Lond.).* 376:203–218.

Cannell, M. B., and D. G. Allen. 1984. Model of calcium movements during activation in the sarcomere of frog skeletal muscle. *Biophys. J.* 45:913–925.

Cecchi, G., F. Colomo, and V. Lombardi. 1981. Force-velocity relation in deuterium oxide-treated frog single muscle fibres during the rise of tension in an isometric tetanus. *J. Physiol. (Lond.).* 317:207–221.

Cleworth, D. R., and K. A. P. Edman. 1972. Changes in sarcomere length during isometric tension development in frog skeletal muscle. *J. Physiol. (Lond.).* 227:1–17.

Cooke, R., M. S. Crowder, C. H. Wendt, V. A. Barnett, and D. D. Thomas. 1984. Muscle cross-bridges: do they rotate? *In* Contractile Mechanisms in Muscle. G. H. Pollack and H. Sugi, editors. Plenum Publishing Corp., New York. 413–423.

Dawson, M. J., D. G. Gadian, and D. R. Wilkie. 1980. Mechanical relaxation rate and metabolism studied in fatiguing muscle by phosphorus nuclear magnetic resonance. *J. Physiol. (Lond.).* 299:465–484.

Duchateau, J., and K. Hainaut. 1986. Nonlinear summation of contractions in striated muscle. II. Potentiation of intracellular Ca^{2+} movements in single barnacle muscle fibres. *J. Musc. Res. Cell Motil.* 7:18–24.

Eisenberg, E., and T. L. Hill. 1985. Muscle contraction and free energy transduction in biological systems. *Science (Wash. DC).* 277:999–1006.

El-Saleh, S. C., K. D. Warber, and J. D. Potter. 1986. The role of tropomyosin-troponin in the regulation of skeletal muscle contraction. *J. Musc. Res. Cell Motil.* 7:387–404.

Eusebi, F., R. Miledi, and T. Takahashi. 1980. Calcium transients in mammalian muscles. *Nature (Lond.).* 284:560–561.

Fryer, M. W., and I. R. Neering. 1986. Relationship between intracellular calcium concentration and relaxation of rat fast and slow muscles. *Neurosci. Lett.* 64:231–235.

Gillis, J. M., D. Thomason, J. Lefèvre, and R. H. Kretsinger. 1982. Parvalbumins and muscle relaxation: a computer simulation study. *J. Musc. Res. Cell Motil.* 3:377–398.

Goldman, Y. E., and R. M. Simmons. 1977. Active and rigor muscle stiffness. *J. Physiol. (Lond.).* 269:55–56.

Goldman, Y. E., M. G. Hibberd, and D. R. Trentham. 1984. Initiation of active contraction by photogeneration of adenosine-5'-triphosphate in rabbit psoas muscle fibres. *J. Physiol. (Lond.).* 354:605–624.

Haselgrove, J., and H. E. Huxley. 1973. X-ray evidence for radial cross-bridge movement and for the sliding filament model in actively contracting skeletal muscle. *J. Mol. Biol.* 77:549–568.

Hibberd, M. G., and D. R. Trentham. 1986. Relationships between chemical and mechanical events during muscular contraction. *Annu. Rev. Biophys. Biophys. Chem.* 15:119–161.

Hill, D. K. 1968. Tension due to interaction between the sliding filaments in resting striated muscle. The effect of stimulation. *J. Physiol. (Lond.).* 199:637–684.

Hill, T. L., E. Eisenberg, and L. Greene. 1980. Theoretical model for the cooperative equilibrium binding of myosin subfragment 1 to the actin-troponin-tropomyosin complex. *Proc. Natl. Acad. Sci. USA.* 77:3186–3190.

Hill, T. L., E. Eisenberg, and J. M. Chalovich. 1981. Theoretical models for cooperative steady-state ATPase activity of myosin subfragment-1 on regulated actin. *Biophys. J.* 35:99–112.

Huxley, A. F. 1957. Muscle structure and theories of contraction. *Prog. Biophys. Biophys. Chem.* 7:255–318.

Huxley, A. F., and R. M. Simmons. 1971. Proposed mechanism of force generation in striated muscle. *Nature (Lond.).* 233:533–538.

Jewell, B. R., and D. R. Wilkie. 1958. An analysis of the mechanical components in frog's striated muscle. *J. Physiol. (Lond.).* 143:515–540.

Kawai, M., and P. W. Brandt. 1980. Sinusoidal analysis: a high resolution method for correlating biochemical reactions with physiological processes in activated skeletal muscles of the rabbit, frog and crayfish. *J. Musc. Res. Cell Motil.* 1:279–303.

Kress, M., H. E. Huxley, A. R. Faruqi, and J. Hendrix. 1986. Structural changes during activation of frog muscle studied by time-resolved x-ray diffraction. *J. Mol. Biol.* 188:325–342.

Mannard, A., and R. B. Stein. 1973. Determination of the frequency response of isometric soleus muscle in the cat using random nerve stimulation. *J. Physiol. (Lond.).* 229:275–296.

Matsubara, I., N. Yagi, and H. Hashizume. 1975. Use of x-ray television for diffraction of the frog striated muscle. *Nature (Lond.).* 255:728–729.

Melzer, W., E. Ríos, and M. F. Schneider. 1986. The removal of myoplasmic free calcium following calcium release in frog skeletal muscle. *J. Physiol. (Lond.).* 372:261–292.

Potter, J. D. 1988. Effect of cross-bridges on the affinity of troponin-C: studies using optical probes. *J. Physiol. (Lond.).* In Press.

Sokolnikoff, I. S., and R. M. Redheffer. 1958. Mathematics of Physics and Modern Engineering. McGraw-Hill Book Co., New York.

Stein, R. B., and F. Parmiggiani. 1981. Nonlinear summation of contractions in cat muscles: I. The early depression. *J. Gen. Physiol.* 78:277–293.

Stein, R. B., and T. Gordon. 1986. Nonlinear stiffness-force relationships in whole mammalian skeletal muscle. *Can. J. Physiol. Pharmacol.* 64:1236–1294.

Stein, R. B., T. Gordon, and J. Shriver. 1982. Temperature dependence of mammalian muscle contractions and ATP activities. *Biophys. J.* 40:97–107.

Stephenson, D. G., and D. A. Williams. 1981. Calcium-activated force responses in fast- and slow-twitch skinned muscle fibres of the rat at different temperatures. *J. Physiol. (Lond.).* 317:281–302.

Zot, A. S., and J. D. Potter. 1987. Structural aspects of troponin-tropomyosin regulation of skeletal muscle contraction. *Annu. Rev. Biophys. Biophys Chem.* 16:535–559.